Low-Temperature Superplastic Behavior of a Submicrometer-Grained 5083 Al Alloy Fabricated by Severe Plastic Deformation

KYUNG-TAE PARK, DUCK-YOUNG HWANG, SI-YOUNG CHANG, and DONG HYUK SHIN

A submicrometer-grained structure was introduced in a commercial 5083 Al alloy by imposing an effective strain of ~8 through equal channel angular pressing. In order to examine the low-temperature superplastic behavior, the as–equal channel angular pressed (as-ECAP) samples were tensile tested in the strain rate range of 10^{-5} to 10^{-2} s^{-1} at temperatures of 498 to 548 K corresponding to 0.58 to 0.65 T_m, where T_m is the incipient melting point. The mechanical data of the alloy at 498 and 548 K exhibited a sigmoidal behavior in a double logarithmic plot of the maximum true stress *vs* true strain rate. The strain rate sensitivity was 0.1 to 0.2 in the low- and high-strain rate regions and 0.4 in the intermediate-strain rate region, indicating the potential for superplasticity. At 523 K, instead of the sigmoidal behavior, a strain rate sensitivity of 0.4 was maintained to low strain rates. A maximum elongation of 315 pct was obtained at 548 K and 5×10^{-4} s^{-1}. The activation energy for deformation in the intermediate-strain rate region was estimated as 63 kJ/mol. Low-temperature superplasticity of the ultrafine grained 5083 Al alloy was attributed to grain boundary sliding that is rate-controlled by grain boundary diffusion, with a low activation energy associated with nonequilibrium grain boundaries. Cavity stringers parallel to the tensile axis were developed during deformation, and the failure occurred in a quasi-brittle manner with moderately diffusive necking.

I. INTRODUCTION

SUPERPLASTICITY refers to the ability of some materials to exhibit an extraordinarily large neck-free elongation prior to failure. In spite of its high potential as a forming technology of complex-shaped components, its application has been limited, since optimum superplasticity generally occurs under the conditions of fine grain sizes (less than 10 μm), high forming temperatures (higher than half of the homologous temperature), and slow forming rates (less than 10^{-3} s^{-1}). In the past decade, in order to overcome the deficiency of the conventional superplasticity, considerable efforts[1] have been devoted in both academic and industrial fields to achieve low-temperature and/or high-strain rate superplasticity by two synergistic motivations: (1) most theories explaining superplasticity predict the possibility of low-temperature and/or high-strain rate superplasticity by further grain refinement, and (2) advanced technologies for fabricating materials with a submicrometer or smaller grain size have been developed.

In the present investigation, a submicrometer-grained (SMG) 5083 Al alloy was processed by equal channel angular pressing, and its low-temperature superplasticity was examined. The 5083 Al alloy is a representative non-age-hardenable Al-Mg based alloy which possesses many interesting characteristics as a structural material, such as low price, moderately high strength, good corrosion resistance, high formability in conjunction with superplasticity, *etc.*[2] These advantages of the alloy are quite attractive in the automobile industry for producing vehicles with high fuel efficiency by replacing steels with the alloy as a body sheet material. In particular, the superplastic property of the alloy provides cost-effectiveness by minimizing the processing steps such as stamping, machining, joining, *etc.* If superplastic forming of the alloy at low temperatures is possible, the cost-effectiveness will be further enhanced by energy savings. Equal channel angular pressing[3,4] is, at present, the most developed severe plastic deformation technique, producing bulk, porosity-free SMG materials. In equal channel angular pressing, a SMG structure is obtained *via* mechanical fragmentation associated with severe plastic deformation by subjecting the sample to repetitive pressing into a die with the two equal cross-sectional channels intersecting at a certain angle. Several previous studies reported low-temperature and/or high-strain rate superplasticity in some equal channel angular pressed (ECAP) SMG materials.[5–8] However, in spite of the engineering significance of the 5083 Al alloy and its low-temperature forming technology, there is still a lack of systematic studies on the low-temperature superplasticity of a SMG 5083 Al alloy produced by equal channel angular pressing, such as the deformation mechanisms based on the relationship between stress and strain rate and the failure mechanisms.

II. EXPERIMENTAL PROCEDURE

A commercial 5083 Al alloy (Al-4.4Mg-0.7Mn-0.15Cr (in wt pct)) was supplied in the form of an extruded bar. Before being ECAP, the alloy was annealed at 723 K for 1 hour and the linear-intercept grain size of the annealed sample was about 200 μm. After machining the cylindrical

KYUNG-TAE PARK, Assistant Professor, and DUCK-YOUNG HWANG, Graduate Assistant, are with the Division of Advanced Materials Science and Engineering, Hanbat National University, Taejon, 305-719, Korea. Contact e-mail: ktpark@hanbat.ac.kr SI-YOUNG CHANG, Assistant Professor, is with the Department of Materials Engineering, Hankuk Aviation University, Kyunggi-Do, 412-791, Korea. DONG HYUK SHIN, Professor, is with the Department of Metallurgy and Materials Science, Hanyang University, Kyunggi-Do, 425-791, Korea.

Manuscript submitted November 20, 2001.

samples of $\phi 10 \times 130$ mm from the annealed bar, an equal channel angular pressing of eight passes was carried out on the samples at 473 K. The present ECAP die was designed to yield an effective strain of ~ 1 by a single pass: the inner contact angle and the arc of curvature at the outer point of contact between channels of the die were 90 and 20 deg, respectively.[9] During equal channel angular pressing, the sample was rotated by 90 deg around its longitudinal axis in the same direction between the passages, *i.e.*, route B_c.[10] It was reported that eight passes of equal channel angular pressing with route B_c resulted in the maximum superplastic elongation among various equal channel angular pressing conditions.[11] The detailed equal channel angular pressing procedure and facility were described elsewhere.[12]

In order to avoid excessive grain growth at the deformation temperatures that could lead to a deterioration in superplastic elongation, the microstructural stability of the ECAP alloy was examined by conducting static annealing at temperatures of 373 to 773 K for 1 hour in either silicone oil or molten salt baths. The annealing temperature was controlled within ± 1 K. As will be discussed later, significant grain growth occurred above 573 K. For superplastic deformation, tensile specimens with a gage length of 8 mm were machined from the as-ECAP bar. Monotonic tensile tests were carried out at initial strain rates of 10^{-5} to 10^{-2} s^{-1} and temperatures of 498 to 548 K on an INSTRON* machine operating at a constant crosshead speed. In some cases, two-step strain rate change tests were done to determine the strain rate sensitivity. While a single specimen was pulled to failure in the monotonic tests, the initial crosshead speed was changed abruptly to the predetermined one in the strain rate change tests after the maximum true stress was confirmed during deformation at the initial crosshead speed.[13] For conventional superplastic materials exhibiting very large uniform elongation, the crosshead speed is usually changed several times in the strain rate change tests. However, in the present study, the crosshead speed was changed only once, since limited ductility was expected at relatively low testing temperatures compared to the conventional superplasticity. All the tests were performed in a three-zone furnace in air, and the testing temperature was controlled within ± 3 K.

*INSTRON is a trademark of Instron Co., Canton, MA.

The microstructure was examined using a JEOL* 2010 transmission electron microscope (TEM) operating at 200 kV. Thin foils for TEM observation were prepared by the twin-jet polishing technique using a mixture of 25 pct nitric acid and 75 pct methanol at an applied potential of 25 V and at 243 K. In addition, the grain structure and cavitation after failure were observed by optical microscopy after etching with dilute Poulton's reagent.

*JEOL is a trademark of Japan Electron Optics Ltd., Tokyo.

III. EXPERIMENTAL RESULTS

A. *Microstructural Stability*

The variation of microhardness with annealing temperature is presented in Figure 1. The microhardness remained virtually constant up to 473 K after a sharp drop at 323 K and then decreased rapidly with increasing annealing temperature in the range of 473 to 573 K, due to recrystallization and subsequent grain growth. It was reported that stress relief in the as-ECAP alloy with extremely high localized stresses by severe plastic deformation can easily occur by substructure rearrangement even at relatively low annealing temperatures:[14,15] for instance, note the rapid loss of hardness at 323 K, as shown in Figure 1. Above 573 K, it remained low and did not change significantly with increasing annealing temperature.

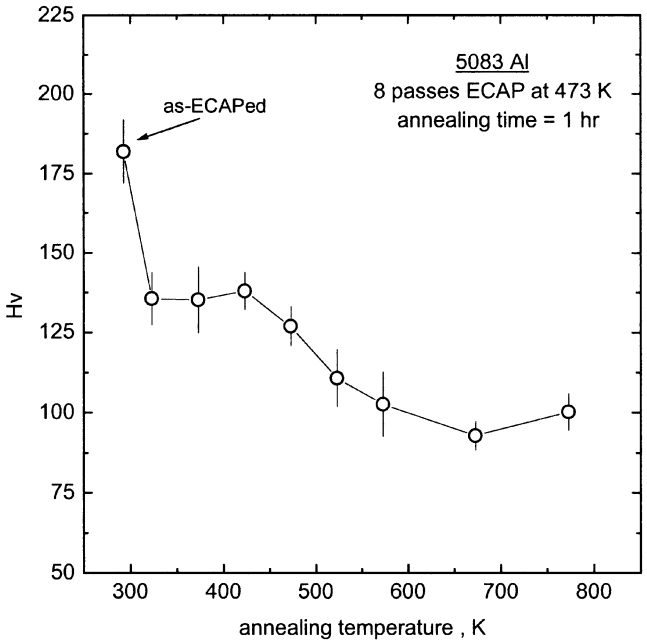

Fig. 1—The variation of microhardness of the eight passes ECAP 5083 Al alloy with annealing temperature.

Figure 2 shows some representative TEM micrographs of the as-ECAP sample and the samples annealed at various temperatures. As typical in SMG materials processed by severe plastic deformation,[16] the as-ECAP sample exhibited ill-defined boundaries and a high dislocation density with dense dislocation debris, *etc.* The average linear-intercept grain size of the as-ECAP sample was about 0.3 μm. Annealing at 473 K did not result in a significant change in the TEM microstructure from that of the as-ECAP sample. At 523 K, dislocation-free recrystallized grains with well-defined grain boundaries appeared, and the grain size distribution became bimodal due to the coexistence of both relatively coarse recrystallized and ultrafine unrecrystallized grains. The microstructure of the sample annealed at 573 K was dominated by very coarse recrystallized grains with a size of several tens of microns. At 573 K, most boundaries were curved, indicating that grain growth was in progress and that a number of particles with a size of 50 to 200 nm and an aspect ratio of 3 to 5 existed in the grain interior. The majority of particles were identified as Al_6Mn intermetallics by chemical analysis with the TEM. It is certain that Al_6Mn particles existed before the sample was ECAP, and their presence, obscured by the ill-defined and ultrafine ECAP structure, became evident when the grain structure

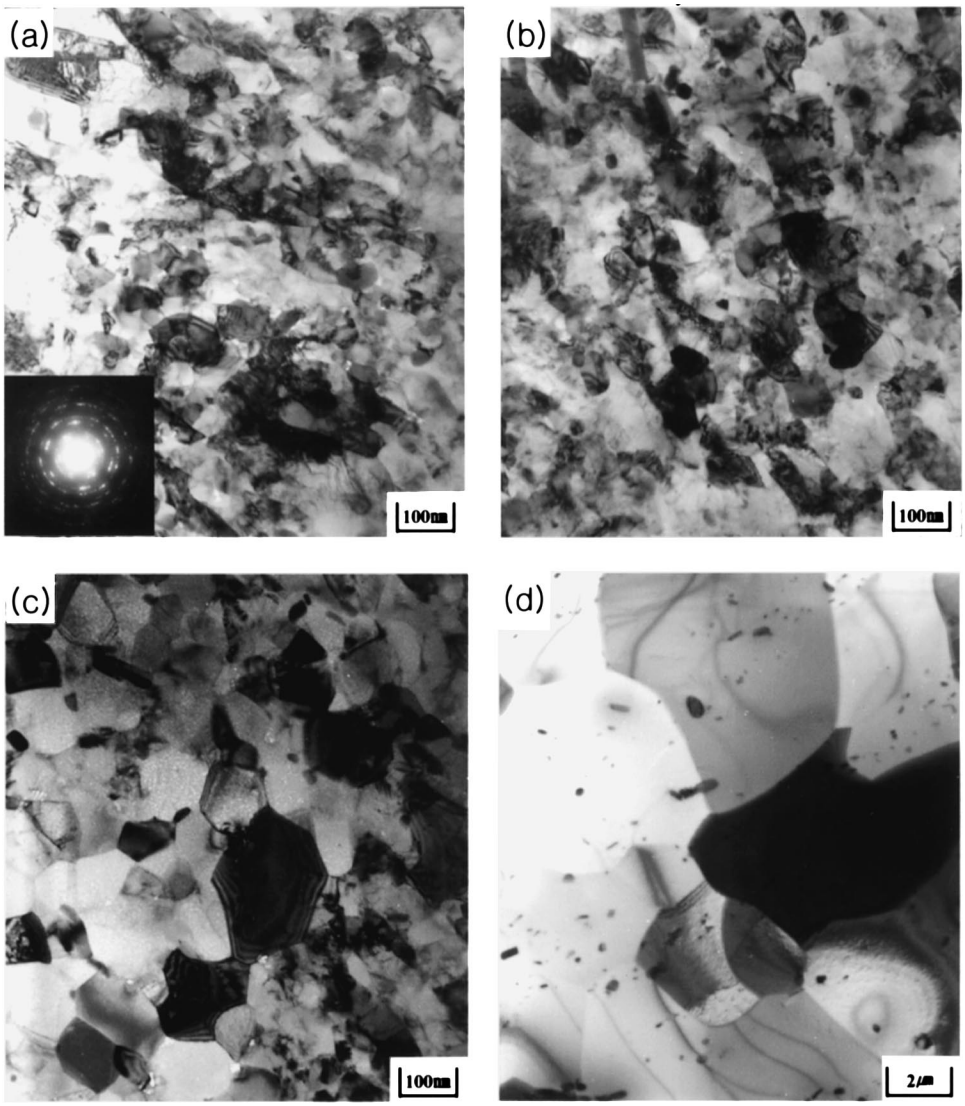

Fig. 2—Representative TEM micrographs of the 5083 Al alloy annealed at various temperatures fo r 1 h after eight passes ECAP: (*a*) as-EACP, (*b*) 473 K, (*c*) 523 K, and (*d*) 573 K.

was well defined by annealing. This microstructural evolution with annealing temperature is well matched with the trend of the microhardness variation shown in Figure 1.

B. *Superplastic Behavior*

1. *Strain rate dependence of flow stress: strain rate sensitivity*

Figure 3 shows a double logarithmic plot of the maximum true flow stresses (σ) *vs* true strain rates ($\dot{\varepsilon}$) for three temperatures of 498, 523, and 548 K. The mechanical data of the alloy at 498 and 548 K exhibited the sigmoidal behavior manifested by the presence of three regions. The strain rate sensitivity ($m = \partial \ln \sigma / \partial \ln \dot{\varepsilon}$) was 0.1 to 0.2 at low (region I, $\dot{\varepsilon} < 10^{-4}\ s^{-1}$) and high (region III, $10^{-3}\ s^{-1} < \dot{\varepsilon}$) strain rates. At the narrow intermediate-strain rate region of one order of magnitude (region II, $10^{-4}\ s^{-1} < \dot{\varepsilon} < 10^{-3}\ s^{-1}$), *m* was about 0.4, indicating the potential for superplasticity. At 523 K, instead of the sigmoidal behavior, region II, with $m = 0.4$, was extended to the lowest strain rate examined and region I was not observed. The present *m* value of 0.4 is higher than that reported previously for low-temperature superplasticity of the same alloy system under similar experimental conditions: 0.2 to 0.3 by Kawazoe *et al.*[17] and 0.3 to 0.4 by Hsiao and Huang.[18]

2. *Temperature dependence of flow stress: activation energy for deformation*

For estimation of the apparent activation energy (Q_a) for deformation, the following expression is often used under the constant stress condition:

$$Q_a = -\,\mathrm{R}\,\frac{\partial \ln \dot{\varepsilon}}{\partial (1/T)} \qquad [1]$$

where $\dot{\varepsilon}$ is the strain rate, R is the universal gas constant, and *T* is the absolute temperature. However, when the strain rate range of interest is narrow, an alternative description for Q_a under the constant strain rate condition is valid:[19]

$$Q_a = n\mathrm{R}\,\frac{\partial \ln \sigma}{\partial (1/T)} \qquad [2]$$

where *n* is the stress exponent that is the reciprocal of *m*.

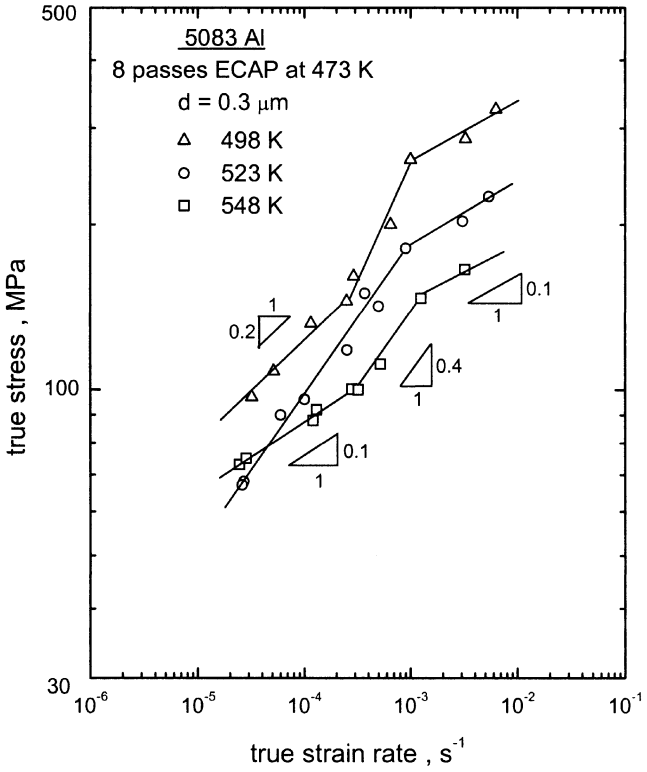

Fig. 3—A double logarithmic plot of true stress *vs* true strain rate of the as-ECAP 5083 Al alloy (eight passes with route B_c) at temperature of 498 to 548 K.

According to Eq. [2], Q_a for regions II and III was estimated from the plot of log σ *vs* 1/*T*, where the slope is equivalent to $Q_a/2.3n\mathrm{R}$. Such a plot is depicted in Figure 4. The value of Q_a was about 61 and 195 kJ/mol at $\dot{\varepsilon} = 5 \times 10^{-4}$ s^{-1} for region II ($n = 2.5$) and at $\dot{\varepsilon} = 3 \times 10^{-3}$ s^{-1} for region III ($n = 8$), respectively. The value of Q_a for region I was not evaluated due to the inconsistent value of the stress exponent at the three testing temperatures. It is worth mentioning that the true activation energy (Q), after compensation for the temperature dependence of the shear modulus, was nearly the same as the apparent value, *i.e.*, 63 and 187 kJ/mol for regions II and III, respectively. The value of Q is expressed by Eq. [3]:[19]

$$Q = \mathrm{R}\,\frac{\partial \ln(\sigma^n/G^{n-1}T)}{\partial(1/T)} \qquad [3]$$

where G is the shear modulus. For calculation of Q, G (MPa) $= 3.2 \times 10^4 - 16T$, where T is in Kelvin, for pure Al[20] was used. The plot related to Eq. [3] is superimposed in Figure 4.

3. *Elongation to failure*

At first, in order to determine the temperature range showing superplastic behavior, tensile tests were carried out on the as-ECAP samples between 473 and 573 K at the initial strain rate of 2×10^{-4} s^{-1}, and the results are shown in Figure 5. While the elongation exceeded 200 pct between 498 and 548 K, with the maximum elongation of 250 pct at 523 K, it was less than 200 pct at 473 and 573 K. As shown in Figure 2, no recrystallization occurred at 473 K, and so a large portion of boundaries still remained low

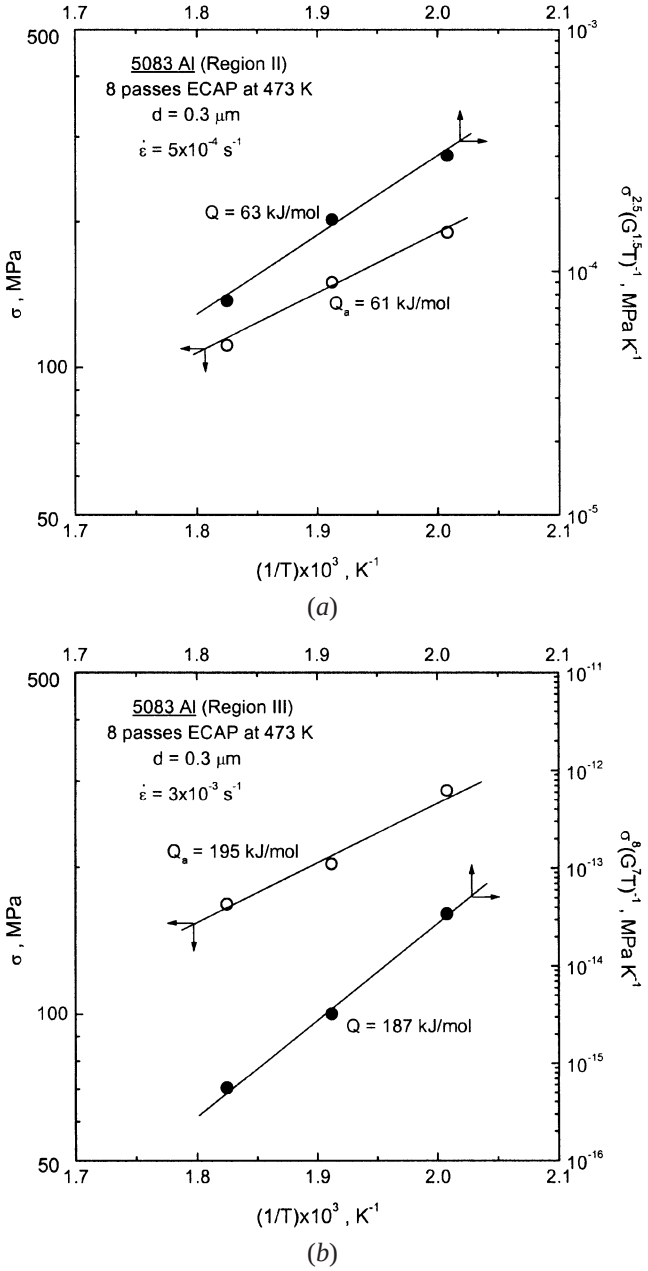

Fig. 4—The plots of log σ and log $(\sigma^n/G^{n-1}T)$ *vs* 1/*T* for the calculation of the activation energy for deformation. (*a*) Region II ($m = 0.4$, $n = 2.5$). (*b*) Region III ($m = 0.12$, $n = 8$).

angled.[10] At 573 K, very coarse recrystallized grains dominated the microstructure. Under these microstructural conditions, superplastic elongation is hardly expected. The strain rate dependence of elongation at the three temperatures of 498, 523, and 548 K is presented in Figure 6. At 498 and 548 K, the maximum elongation was obtained at the strain rate range of 10^{-4} to 10^{-3} s^{-1}, which corresponds to region II in Figure 3. In particular, beyond 5×10^{-4} s^{-1}, the elongation at 548 K was larger than that at the other two temperatures. At 523 K, a high elongation of about 250 pct was obtained even at the lowest strain rate of 5×10^{-5} s^{-1}, this being attributed to the high m value being extended to low strain rates at this temperature, as shown in Figure 3. Among all testing conditions, a maximum elongation of 315 pct was obtained at 548 K and 5×10^{-4} s^{-1}.

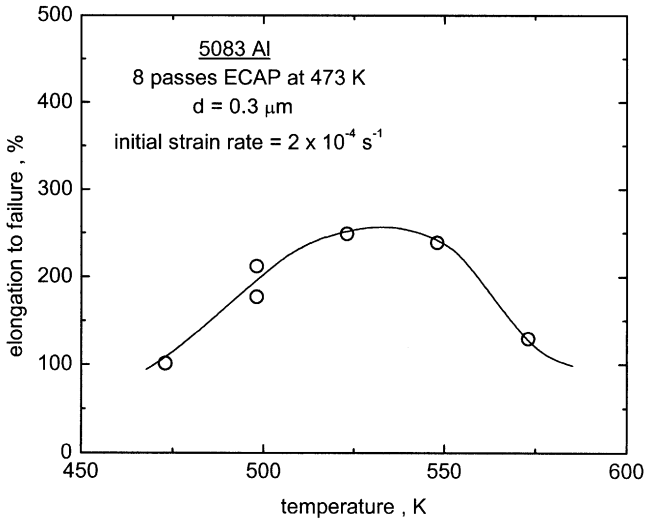

Fig. 5—Elongation to failure of the as-ECAP 5083 Al alloy (eight passes with route B_c) at temperatures of 473 to 573 K. The initial strain rate was 2×10^{-4} s^{-1}.

4. *Cavitation*

The fractured samples tested at various initial strain rates at 548 K are shown in Figure 6(b). The samples broke in a quasi-brittle manner with moderately diffusive necking, indicating the occurrence of cavitation. Figures 7(a) and 7(b) present optical micrographs of the fracture tip and the gage section of the sample, respectively, tested at 548 K and the initial strain rate of 5×10^{-4} s^{-1}. Extensive cavitation is evident at the fracture tip. It is of interest to note that cavities developed in the form of stringers parallel to the tensile axis at both locations, having different local strains. The formation of cavity stringers parallel to the tensile axis is commonly observed in conventional superplastic materials, and several mechanisms for their formation have been suggested elsewhere.[21,22]

IV. DISCUSSION

A. *The Mechanical Behavior of the ECAP SMG 5083 Al Alloy*

Except at 523 K, where region II, showing a high *m* value, extends to low strain rates, the stress dependence of the strain rate of the ECAP SMG 5083 Al alloy at 498 and 548 K is characterized by a sigmoidal behavior, as shown in Figure 3. The sigmoidal behavior is generally observed in conventional (high-temperature) superplasticity. In addition, Neishi *et al.*[7] recently observed this behavior in the low-temperature superplasticity of an ECAP Cu-Zn-Sn alloy. Region III (high strain rate region), with a low *m* value, is often explained by the breakdown of the power-law creep. Region II (intermediate strain rate region) is called the superplastic region, where the maximum elongation is obtained and grain boundary sliding governs the deformation. However, the origin of region I (low strain rate region), with a low *m* value, is still in controversy.

1. *High strain rate region (region III)*

The deformation behavior of the present alloy in the high strain rate region is characterized by $m = 0.12$ ($n = 8$) and $Q = 187$ kJ/mol. This behavior does not match with any

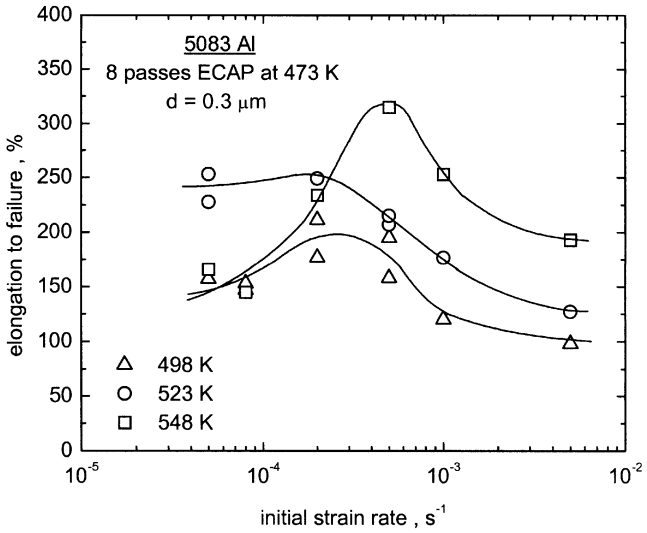

(*a*)

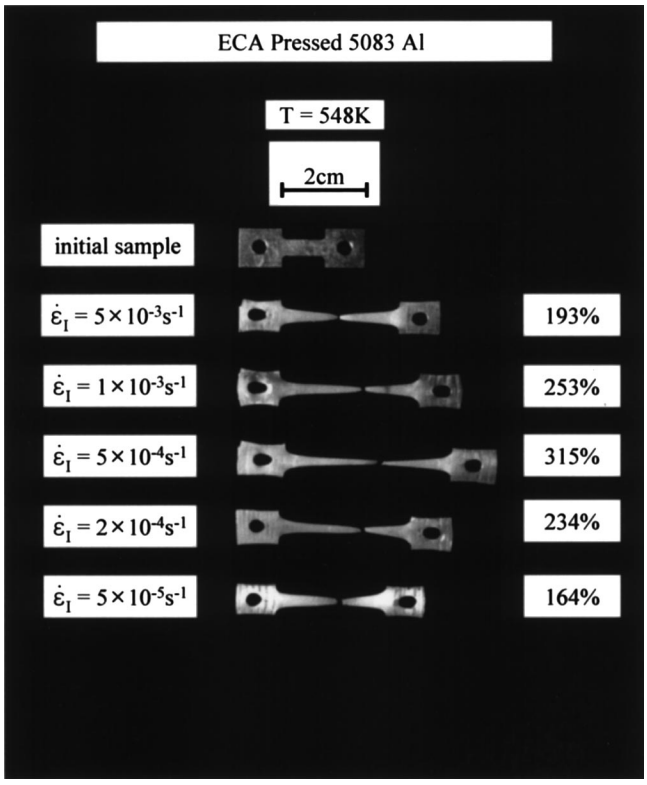

(*b*)

Fig. 6—(*a*) The variation of elongation to failure with the initial strain rate at temperatures of 498 to 548 K. (*b*) Appearance of the sample pulled to failure at the various initial strain rate ($T = 548$ K).

standard deformation mechanisms with the power law, suggesting that the experiment was carried out in the power-law breakdown region. Although the *n* value (equal to 8) is close to that predicted from the lattice diffusion controlled creep with a constant structure,[23] *Q* (equal to 187 kJ/mol) is higher than the activation energy for lattice diffusion of Al (142 kJ/mol). Sherby and Burke[24] proposed that power-law breakdown in the deformation of fcc materials occurs at a diffusivity-normalized strain rate of $\dot{\varepsilon}/D = 10^{13}$ m^{-2}, where *D* is the appropriate diffusivity. In the present case,

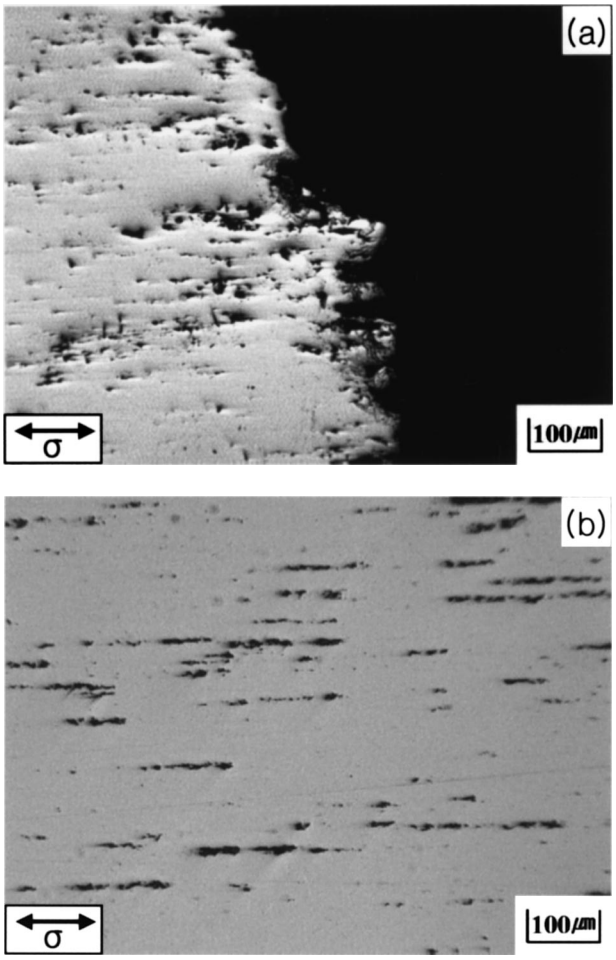

Fig. 7—Cavitation in the as-ECAP 5083 Al alloy (eight passes with route B_c) tested at 548 K and 5×10^{-4} s^{-1}. (*a*) fracture tip and (*b*) gage section.

the critical $\dot{\varepsilon}$ level showing the transition from region II to region III is about 10^{-3} s^{-1}, as shown in Figure 3. When $D = 1.24 \times 10^{-4} \exp(-130{,}500/RT)$ ($m^2 s^{-1}$) for Mg diffusion in Al[25] was used, since Mg is the major alloying element of the 5083 Al alloy, the present $\dot{\varepsilon}/D$ values being 3.9×10^{14} m^{-2} at 498 K, 8.7×10^{13} m^{-2} at 523 K, and 2.2×10^{13} m^{-2} at 548 K. These values are comparable to the value suggested by Sherby and Burke. Accordingly, the present region III is likely to represent the power-law breakdown behavior.

2. *Intermediate strain rate region (region II)*

The *m* value of 0.4 in region II is comparable to that of 0.5 predicted by the grain boundary sliding mechanism. The activation energy for superplastic deformation associated with grain boundary sliding is usually close to that for grain boundary diffusion. Besides, in some coarse grained Al-Mg alloys[26,27,28] showing extended ductility at testing temperatures similar to the present study, the activation energy was reported to be close to that for Mg diffusion in Al (130 to 140 kJ/mol): deformation in these alloys was associated with solute-dragged dislocation glide rather than grain boundary sliding. In the present case, the activation energy in region II (Q = 63 kJ/mol) was lower than that for grain boundary diffusion (Q_{gb}) of Al (86 kJ/mol)[25] and of Mg diffusion in Al. An explanation is needed for this discrepancy. Very recently, Kolobov *et al.*[29] found that the

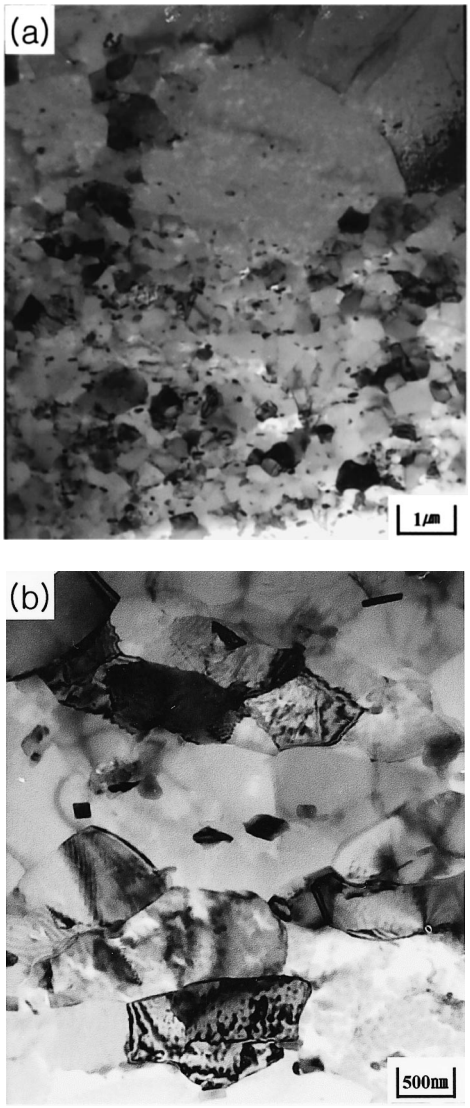

Fig. 8—TEM micrographs taken from the gage section of the samples tested at 523 K and 5×10^{-4} s^{-1} (region II). (*a*) Low magnification showing the bimodal distribution of the grain size. (*b*) High magnification showing the presence of nonequilibrium grain structure.

Q_{gb} value of ECAP Ni was much lower than that of coarse grained Ni and was close to the activation energy of free-surface diffusion due to the nonequilibrium nature of grain boundaries induced by severe plastic deformation. In order to check this possibility, the microstructures of the sample deformed in region II were examined by the TEM. Figure 8 shows TEM micrographs taken from the gage section of the fractured samples tested at 523 K and the initial strain rate of 5×10^{-4} s^{-1}. The bimodal distribution of the grain size was evident in Figure 8(a). The coarse grains, of course, resulted from continuous recrystallization and subsequent grain growth during deformation. The fine grains, magnified in Figure 8(b), consisted of recovered grains and unrecovered grains with a high dislocation density and ill-defined grain boundaries. It indicates that a certain portion of the grain structure remained in nonequilibrium during deformation and, therefore, a Q_{gb} value lower than that in an equilibrium structure is expected in the present alloy, as pointed out by Kolobov *et al.*[29] Accordingly, it is quite probable that region

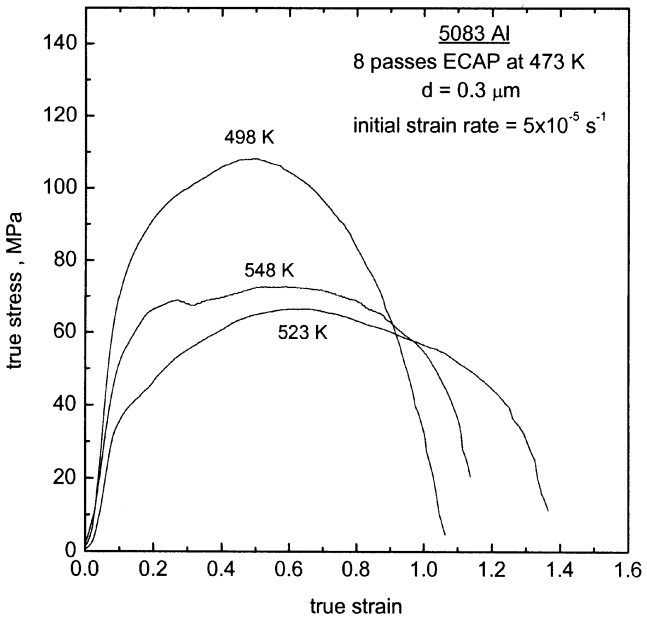

Fig. 9—The true stress–true strain curves of the as-ECAP 5083 Al alloy (eight passes with route B_c) tested with the initial strain rate of 5×10^{-5} s^{-1} belonging to region I at various testing temperatures.

II deformation is governed by grain boundary sliding rate controlled by grain boundary diffusion with a low activation energy associated with the nonequilibrium nature of grain boundaries.

3. *Low strain rate region (region I)*

Several different mechanisms have been suggested for explaining the deformation behavior of superplastic alloys in region I, such as the sequential operation of two deformation mechanisms,[30] the existence of threshold stress associated with impurity segregation at grain boundaries,[31] the microstructural evolution during high temperature deformation such as concurrent grain growth,[32] *etc.* The first two suggestions predict either a consistent *m* value at all testing temperatures or a devement of the *m* value with decreasing stress at a single testing temperature, respectively. By contrast, the *m* value in the present study was not consistent at the three testing temperatures, but it remained constant at a single testing temperature. Accordingly, the microstructural evolution during deformation is the most likely cause of the region I deformation behavior.

Figure 9 shows the true stress–true strain curves of the as-ECAP 5083 Al alloy tested with the initial strain rate of 5×10^{-5} s^{-1} belonging to region I at the three testing temperatures. At 498 K, a rapid strain hardening occurred from the initial stage of deformation, showing the maximum stress at true strain of ~0.4. The rapid initial strain hardening is generally observed in strain-hardened materials having a high dislocation density.[33] From Figures 1 and 2, it is seen that recrystallization occurred partially at 498 K. Therefore, a considerable portion of grain boundaries still remained low angled, and dislocations were in high density, although recovery was in progress. That makes grain boundary sliding difficult, causing the low *m* value in this region. The same microstructural explanation can be applied to a relatively low elongation less than 200 pct at 498 K, even in region II with $m = 0.4$. This fact can be confirmed by the micrographs taken from the gage section of the sample which

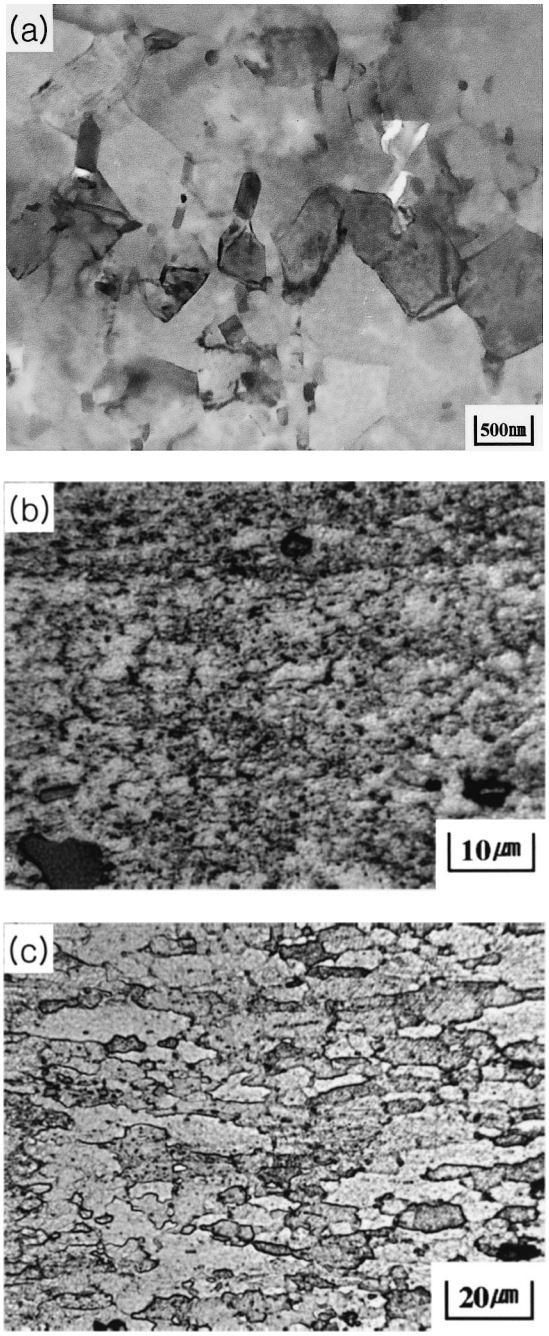

Fig. 10—The microstructure of the gage section of the samples tested to failure at initial strain rate of 5×10^{-5} s^{-1} (region I). (*a*) 498 K (TEM), (*b*) 523 K (OM), and (*c*) 548 K (OM).

failed with the initial strain rate of 5×10^{-5} s^{-1}. As shown in Figure 10(a), the microstructure of the sample fractured at 498 K consisted of recrystallized grains with a size of ~1 μm and unrecrystallized ultrafine grains with ill-defined grain boundaries. A gradual strain hardening was observed at 523 and 548 K, with the maximum stress at true strain of ~0.6. This resulted from the occurrence of concurrent recrystallization followed by grain growth.[33,34] From Figure 10(b), showing the microstructure of the sample tested until failure at 523 K, which was etched with dilute Poulton's reagent to effectively reveal the high angle boundaries,[35] it is seen that a large portion of the microstructure consisted

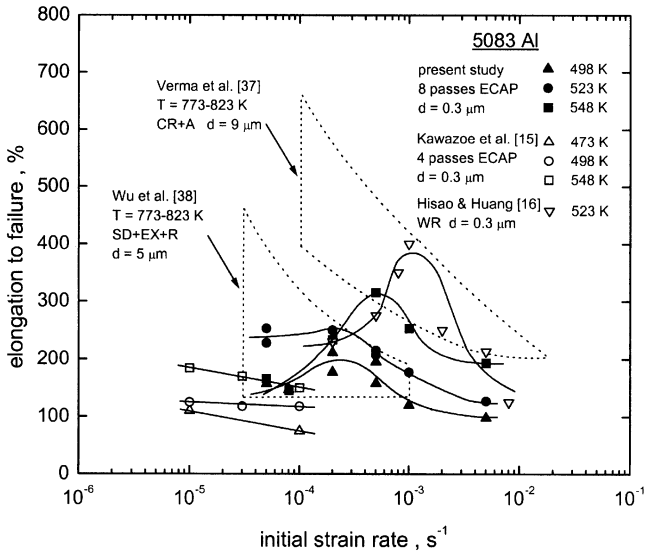

Fig. 11—The comparison of the elongation data of low-temperature superplasticity of 5083 Al alloy. The data of conventional (high temperature) superplasticity of the same alloy are also presented. (SD—spray deposition, EX—extrusion, R—rolling, CR—cold rolling, A—annealing, and WR—warm rolling).

of recrystallized grains of ~5 μm. This grain size was enough to show superplasticity and resulted in the relatively high elongation exceeding 250 pct and high *m* value, *i.e.*, the absence of region I at this temperature. At 548 K (Figure 10(c)), significant grain growth occurred and the grain size was ~20 μm, too large for superplasticity, causing the low *m* value and low elongation.

B. *Low-temperature superplasticity of an ECAP SMG 5083 Al alloy*

The elongation data of the present SMG 5083 Al alloy are compared to those reported from other previous investigations[17,18,36,37] in Figure 11. The data for the conventional superplastic 5083 Al alloy,[36,37] *i.e.*, high temperatures and a grain size of the order of several micrometers, are also included in the figure. Several findings are noted. First, in spite of a slight difference in chemical composition, the eight-passes ECAP 5083 Al alloy exhibited larger elongation at higher strain rates compared to the four-passes ECAP 5056 Al alloy[17] under a similar grain size and deformation temperatures. It was reported that, with increasing equal channel angular pressing strain, a portion of high-angled grain boundaries increases but the grain size virtually remains unchanged.[17,18] This microstructural evolution during equal channel angular pressing may lead to the increase of the grain boundary sliding contribution associated with high-angled grain boundaries to overall deformation. It resulted in larger elongation of the eight-passes ECAP 5083 Al alloy at higher strain rates. Second, the elongation of the eight-passes ECAP 5083 Al alloy was inferior to that of the warm-rolled (WR) 5083 Al alloy reported by Hisao and Huang.[18] In their study, the maximum elongation of ~400 pct was obtained at 523 K and 1×10^{-3} s^{-1}, but the maximum elongation of 315 pct was obtained at 548 K and 5×10^{-4} s^{-1} in the present study. This may be ascribed to the difference in texture development during materials processing between the WR and ECAP samples. For the present case, the sample was rotated by 90 deg around its longitudinal axis in the same direction between the passages, and so a less textured microstructure was expected as compared to the WR sample. Hisao and Huang[18] reported that elongation of the WR 5083 Al samples machined parallel to the rolling direction was much better than that of the samples machined perpendicular to the rolling direction. This fact lends support to the explanation of the elongation difference between the ECAP and WR samples in terms of texture. Finally, as shown in Figure 11, the elongation data of low-temperature superplasticity induced by a SMG structure are quite overlapped with those of conventional (high temperature) superplasticity in the relatively high strain rate range, *i.e.*, 10^{-4} to 10^{-2} s^{-1}. It indicates the engineering significance of grain refinement in this alloy system in view of low-temperature forming process.

V. CONCLUSIONS

1. The low-temperature superplasticity of a submicrometer-grained (≈0.3 μm) 5083 Al alloy fabricated by equal channel angular pressing was examined at temperatures of 498, 523, and 548 K and $\dot{\varepsilon} = 10^{-5}$ to 10^{-2} s^{-1}.
2. The mechanical data of the alloy at 498 and 548 K exhibited the sigmoidal behavior in a double logarithmic plot of the maximum true stress *vs* the corresponding true strain rate. While the strain rate sensitivity was 0.1 to 0.2 at low- and high-strain rate regions, it was ~0.4 in the intermediate strain rate region. At the intermediate strain rate region, the activation energy for deformation was ~63 kJ/mol. However, at 523 K, the strain rate sensitivity of 0.4 was maintained at low strain rates.
3. The analysis indicated that the low-temperature superplasticity of the present ultrafine grained alloy was attributed to grain boundary sliding that is rate controlled by grain boundary diffusion with a low activation energy associated with the nonequilibrium nature of grain boundaries.
4. Below $\dot{\varepsilon} = 5 \times 10^{-4}$ s^{-1}, the elongation at 523 K was larger than that at the other two temperatures, due to the high strain rate sensitivity value. But, above $\dot{\varepsilon} = 5 \times 10^{-4}$ s^{-1}, the elongation at 548 K was larger than that at the other two temperatures, with the maximum elongation of 315 pct at $\dot{\varepsilon} = 5 \times 10^{-4}$ s^{-1}.
5. Cavity stringers parallel to the tensile axis developed during deformation, and the failure occurred in a quasi-brittle manner with moderately diffusive necking.

ACKNOWLEDGMENTS

This work was supported by the Korea Ministry of Science and Technology through the "2000 National Research Laboratory Program."

REFERENCES

1. *Towards Innovations in Superplasticity II, JIMIS 9*, Kobe, Japan, T. Sakuma, T. Aizawa, and K. Higashi, eds., Trans Tech Pub., Aedermannsdorf, Switzerland, 1999.
2. R.L. Hecht and K. Kannan: in *Superplasticity and Superplastic Forming*, A.K. Gosh and T.R. Bieler, eds., TMS, Warrendale, PA, 1995, pp. 259-64.

3. V.M. Segal, V.I. Reznikov, A.D. Drobyshevsky, and V.I. Kopylov: *Russ. Metall.*, 1981, vol. 1, pp. 99-105.
4. V.M. Segal: *Mater. Sci. Eng.*, 1995, vol. A197, pp. 157-64.
5. R.Z. Valiev, D.A. Salimonenko, N.K. Tsenev, P.B. Berbon, and T.G. Langdon: *Scripta Mater.*, 1997, vol. 37, pp. 1945-50.
6. Z. Horita, M. Furukawa, M. Nemoto, A.J. Barnes, and T.G. Langdon: *Acta Mater.*, 2000, vol. 48, pp. 3633-40.
7. K. Neishi, T. Uchida, A. Yamauchi, K. Nakamura, Z. Horita, and T.G. Langdon: *Mater: Sci. Eng.*, 2001, vol. A307, pp. 23-28.
8. S.Y. Chang, J.G. Lee, K.-T. Park, and D.H. Shin: *Mater. Trans. (JIM)*, 2001, vol. 42, pp. 1074-80.
9. Y. Iwahashi, J. Wang, Z. Horita, M. Nemoto, and T.G. Langdon: *Scripta Mater.*, 1996, vol. 35, pp. 143-46.
10. M. Nemoto, Z. Horita, M. Furukawa, and T.G. Langdon: *Metall. Mater.*, 1998, vol. 4, pp. 1181-90.
11. S. Komura, M. Furukawa, Z. Horita, M. Nemoto, and T.G. Langdon: *Mater. Sci. Eng.*, 2001, vol. A297, pp. 111-18.
12. D.H. Shin, B.C. Kim, Y.-S. Kim, and K.-T. Park: *Acta Mater.*, 2000, vol. 48, pp. 2247-55.
13. J. Pilling and N. Ridley: *Superplasticity in Crystalline Solids*, The Institute of Metals, London, 1989, p. 28
14. S. Komura, Z. Horita, M. Nemoto, and T.G. Langdon: *J. Mater. Res.*, 1999, vol. 14, pp. 4044-51.
15. Y.M. Yang, E. Ma, and M.W. Chen: *Appl. Phys. Lett.*, 2002, vol. 80 (13), pp. 2395-97.
16. R.Z. Valiev, R.K. Islamgaliev, and I.V. Alexandrov: *Progr. Mater. Sci.*, 2000, vol. 45, pp. 103-89.
17. M. Kawazoe, T. Shibata, T. Mukai, and K. Higashi: *Scripta Mater.*, 1997, vol. 36, pp. 699-705.
18. I.C. Hisao and J.C. Huang: *Scripta Mater.*, 1999, vol. 40, pp. 697-703.
19. F.A. Mohamed and T.G. Langdon: *Phys. Status Solidi*, 1976, vol. 33, pp. 375-81.
20. J.E. Bird, A.K. Mukherjee, and J.E. Dorn: in *Quantitative Relation between Properties and Microstructures*, D.G. Brandon and A. Rosen, eds., Israel University Press, Jerusalem, 1969, p. 255
21. K.-T. Park, J.C. Earthman, and F.A. Mohamed: *Phil. Mag. Lett.*, 1994, vol. 70, pp. 7-13.
22. D.H. Shin and K.-T. Park: *Mater. Sci. Eng.*, 1999, vol. A268, pp. 55-62.
23. O.D. Sherby, R.H. Klundt, and A.K. Miller: *Metall. Trans. A*, 1977, vol. 8A, pp. 843-52.
24. O.D. Sherby and P.M. Burke: *Progr. Mater. Sci.*, 1967, vol. 13, pp. 325-90.
25. S.J. Rothman, N.J. Peterson, L.J. Lowicki, and L.C. Robinson: *Phys. Status Solidi*, 1974, vol. B63, p. 29.
26. T.R. McNelly, E.W. Lee, and M.E. Mills: *Metall. Trans. A*, 1986, vol. 17A, pp. 1035-41.
27. S.S. Woo, Y.R. Kim, D.H. Shin, and W.J. Kim: *Scripta Mater.*, 1997, vol. 37, pp. 1351-58.
28. E.M. Taleff, G.A. Hanshall, T.G. Nieh, D.R. Lesuer, and J. Wadsworth: *Metall. Mater. Trans. A*, 1998, vol. 29A, pp. 1081-91.
29. Y.R. Kolobov, G.P. Grabovetskaya, M.B. Ivanov, A.P. Zhilyaev, and R.Z. Valiev: *Scripta Mater.*, 2001, vol. 44, pp. 873-78.
30. F.A. Mohamed and T.G. Langdon: *Phil. Mag.*, 1975, vol. 32, pp. 697-709.
31. P.K. Chaudhury and F.A. Mohamed: *Acta Metall.*, 1988, vol. 36, pp. 1099-1110.
32. G. Rai and N.J. Grant: *Metall. Trans. A*, 1975, vol. 6A, pp. 385-90.
33. Z. Horita, T. Fujinami, M. Nemoto, and T.G. Langdon: *Metall. Mater. Trans. A*, 2000, vol. 31A, pp. 691-701.
34. H. Iwasaki, S. Hayami, K. Higashi, and S. Tanimura: in *Superplasticity in Metals, Ceramics and Intermetallics*, Proc. MRS, M. Mayo, M. Kobayashi, and J. Wadsworth, eds., Pittsburgh, PA, 1990, pp. 233-38.
35. G. Petzow: *Metallographic Etching*, ASM, Metals Park, OH, 1978, p. 39.
36. R. Verma, A.K. Gosh, S. Kim, and C. Kim: *Mater. Sci. Eng.*, 1995, vol. A191, pp. 143-50.
37. Y. Wu, L.D. Castillo, and E.J. Lavernia: *Metall. Mater. Trans. A*, 1997, vol. 28A, pp. 1059-68.
38. Y. Iwashashi, Z. Horita, M. Nemoto, and T.G. Langdon: *Acta Mater.*, 1998, vol. 46, pp. 3317-31.